Methods and mechanisms for improving combustion stability by fluid recirculation structures in micro-structured burners

Christopher Brown [a], Junjie Chen [a, b, c, *]

[a] Department of Mechanical and Aerospace Engineering, College of Engineering, University of California, Davis, California, 95616, United States

[b] Department of Automotive Engineering, School of Mechanical and Automotive Engineering, South China University of Technology, Guangzhou, Guangdong, 510641, P.R. China

[c] Department of Energy and Power Engineering, School of Mechanical and Power Engineering, Henan Polytechnic University, Jiaozuo, Henan, 454000, P.R. China

* Corresponding author. E-mail address: junjiem@tom.com

Abstract

A combustion air stream is introduced tangentially into the interior of a premix burner by means of a swirl producer, and is mixed with fuel. At the burner outlet, the vortex flow which arises bursts open at a sudden change of cross section, with the initiation of a back-flow zone which serves to stabilize a flame in the operation of the burner. Although premix burners make possible an operation with very low pollutant emissions, they often operate dangerously near to the extinction limit of the flame. Cavity structures have been designed for the purpose of improving flame stability. However, the precise mechanism by which the cavity method provides increased flame stability remains unclear. This study relates to the combustion characteristics and flame stability of a micro-structured cavity-stabilized burner. Computational fluid dynamics simulations are conducted to gain insights into burner performance such as reaction rates, species concentrations, temperatures, and flames. Factors affecting combustion characteristics and flame stability are determined. Design recommendations are provided. The results indicate that the thermal conductivity of the burner walls plays a vital role in flame stability. Improvements in flame stability are achievable by using walls with anisotropic thermal conductivity. Heat-insulating materials are favored to minimize external heat losses. Burner dimensions greatly affect flame stability. The inlet velocity of the mixture is a critical factor in assuring flame stability within the cavity-stabilized burner. There is a narrow range of inlet velocities that permit sustained combustion within the cavity-stabilized burner. There are issues of efficiency loss for fuel-rich cases. Burners with large dimensions lead to a delay in flame ignition and may cause blowout. The combustion is stabilized by recirculation of hot combustion products induced by the cavity structure.

Keywords: Reaction rates; Species concentrations; Temperatures; Flames; Burners; Combustion

1. Introduction

Compact, highly mobile, and efficient thermodynamic and energy systems are becoming increasingly important for a wide range of applications [1, 2], such as thermodynamic cycling of distributed ventilation and heating systems, modular propulsion and control of self-powered and distributed sensor and actuation systems [3, 4], and cooling and powering of portable communications and electronics devices [5, 6], and many other applications. Generally, such applications optimally require power sources that are cost effective, and that are characterized by high energy density and power [7, 8] but minimal weight and dimensions.

Micro-structured combustion systems may overcome limitations of traditional thermodynamic and power sources [9, 10] by providing micromachinery components that enable efficient operation of thermodynamic systems and production of significant power in the regime of millimeters [11, 12] to meet the cost, weight, modularity, mobility, and efficiency requirements of a wide range of modern applications. For example, micro-structured combustion systems can provide power sources that can be employed in a wide range of portable electric power applications [13, 14] such as portable coolers, heaters, communication and electronic devices, and other such applications.

More particularly, micro-structured combustion systems enable realization of a wide range of micromachinery componentry for thermodynamic cycling, propulsion, and producing sources of power that achieve high efficiencies of components at sizes on the order of millimeters [15, 16]. Micro-heat exchangers [17, 18], micro-pumps, micro-turbines, micro-combustors [19, 20], micro-compressors, and other micro-componentry can be developed as thermodynamic micro-modules that could be interconnected in various combinations to construct micro-structured thermodynamic cycles such as micro-gas turbine generators [21, 22], micro-gas turbine engines [23, 24], and a wide range of other thermodynamic cycles, for example, for circulation, propulsion [25, 26], cooling, heating, and other applications in the regime of millimeters.

Specifically, micro-structured combustion systems are applicable to all portable electric power applications for which air is available [27, 28]. This includes, for example, radios, portable computers, and other electronic devices; telephones, for example, cellular telephones, and other communication devices; coolers and heaters, power tools, military weapons, for example, missiles, as well as many other applications. The very low noise produced by micro-structured combustion systems makes them particularly attractive from a practical perspective for applications such as military reconnaissance and office electronics [29, 30]. Micro-structured combustion systems can be further advantageously employed in manned mobile scenarios, for example, fire-fighting. More particularly, individual power packs of micro-structured combustion systems can be provided to fire fighters for mobile, autonomous powering of communication apparatus and personal protection [31, 32]. Micro-structured combustion systems can similarly be employed to power implanted medical devices, for example, pace makers.

Unfortunately, flame stabilization is a common problem in micro-structured combustion systems [33, 34]. Various attempts have been made to achieve improvements in flame stability. More specifically, various methods have been tried either commercially or experimentally [35, 36] and many different structures have already been designed for micro-structured combustion systems [37, 38]. The typical method includes the use of recirculation regions to provide a continuous ignition source by mixing the hot combustion products with the cold incoming fuel and air mixture. Structural devices have been commonly employed to establish a recirculation region for improving the stability of the flame during ignition and operation, for example, cavities [39, 40]. A fundamental understanding of the stabilization mechanisms of a flame within very small spaces by the cavity method is of both fundamental and practical significance. However, the precise mechanism by which the cavity method generally provides increased flame stability remains unclear and warrants further study.

This study relates to the combustion characteristics and flame stability of a micro-structured cavity-stabilized burner. Computational fluid dynamics simulations are conducted to gain insights into burner performance such as reaction rates, species concentrations, temperatures, and flames. The factors affecting combustion characteristics and flame stability are determined for the cavity-stabilized burner. The objective is to investigate the combustion characteristics and flame stability of micro-structured cavity-stabilized combustion systems. Particular focus is placed on determining essential factors that affect the combustion characteristics and flame stability of the systems.

2. Description of the model

2.1. Description of the combustion system

The use of a cavity configuration is particularly advantageous when arranged as a disturbance factor for millimeter-scale combustion systems. Therefore, such a configuration is employed in the present study. The millimeter-scale combustion system designed with cavities is depicted schematically in Figure 1 with the solution domain indicated. A lean methane-air mixture is conducted through a combustion chamber defined by parallel plates. The length of the channel is 50 mm, the height is 3 mm, and the width is 13 mm. The depth of the cavities is 1.5 mm, the width of the cavities is 4 mm, and the distance away from the entrance is 10 mm. The angle of the cavity is 45°, and the thickness of the plates is 3 mm, as depicted schematically in Figure 1. The initial temperature of the premixed mixture is 1500 K, with a Reynolds number greater than 500 at the inlet. Due to the small internal space of the burner, the gas flow rate is small. Therefore, gas radiation and volume force are ignored in the model.

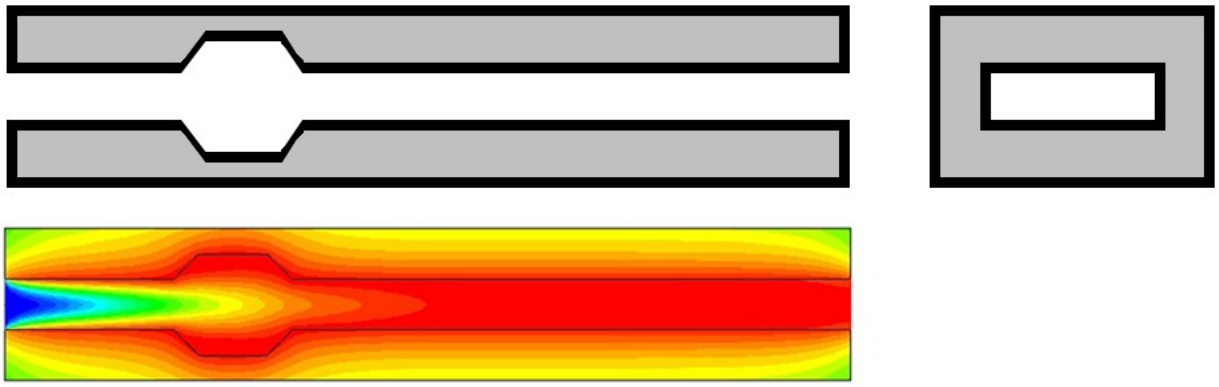

Figure 1. Schematic illustration of the millimeter-scale combustion system designed with cavities on the channel walls with the solution domain indicated.

2.2. Mathematical model

The mathematical model is solved and implemented in ANSYS FLUENT to obtain the problem solution. ANSYS FLUENT permits multi-dimensional modeling of physical and chemical phenomena in the processes [41, 42], and various modes of heat transfer can be modeled.

The continuity equation is given by

$$\frac{\partial}{\partial x}(\rho v_x) + \frac{\partial}{\partial y}(\rho v_y) = 0, \tag{1}$$

where v_x is the velocity along the x-axis, v_y is the velocity along the y-axis, and ρ is the density.

The momentum conservation equations can be written as

$$\frac{\partial(\rho v_x v_x)}{\partial x} + \frac{\partial(\rho v_x v_y)}{\partial y} = -\frac{\partial p}{\partial x} + \frac{\partial \tau_{xx}}{\partial x} + \frac{\partial \tau_{xy}}{\partial y}, \tag{2}$$

$$\frac{\partial(\rho v_y v_x)}{\partial x} + \frac{\partial(\rho v_y v_y)}{\partial y} = -\frac{\partial p}{\partial y} + \frac{\partial \tau_{yx}}{\partial x} + \frac{\partial \tau_{yy}}{\partial y}, \tag{3}$$

where τ is the stress tensor.

The energy conservation equation is given by

$$\frac{\partial(\rho v_x h)}{\partial x}+\frac{\partial(\rho v_y h)}{\partial y}=\frac{\partial(k_{ff}\partial T)}{\partial x^2}+\frac{\partial(k\ \partial T)}{\partial y^2}+\sum_i\left[\frac{\partial}{\partial x}\left(h_i\rho D_{i,m}\frac{\partial Y_i}{\partial x}\right)+\frac{\partial}{\partial y}\left(h_i\rho D_{i,m}\frac{\partial Y_i}{\partial y}\right)\right]+\sum_i h_i R_i \quad (4)$$

where h is the enthalpy, k_f is the thermal conductivity of the fluid, T is the temperature, $D_{i,m}$ is the molecular diffusivity of species i, Y is the mass fraction, and R is the reaction rate.

The species conservation equation can be written as

$$\frac{\partial(\rho Y_i v_x)}{\partial x}+\frac{\partial(\rho Y_i v_y)}{\partial y}=\frac{\partial}{\partial x}\left(\rho D_{i,m}\frac{\partial Y_i}{\partial x}\right)+\frac{\partial}{\partial y}\left(\rho D_{i,m}\frac{\partial Y_i}{\partial y}\right)+R_i. \quad (5)$$

The energy conservation equation of the solid phase can be written as

$$\frac{\partial}{\partial x}\left(k_s\frac{\partial T}{\partial x}\right)+\frac{\partial}{\partial y}\left(k_s\frac{\partial T}{\partial y}\right)=0, \quad (6)$$

where k_s is the thermal conductivity of the solid wall.

2.3. Chemical kinetic model

Based on the finite rate chemical reaction model using Arrhenius's law, the expression of the rate of the gas phase combustion reaction can be written as follows [43]:

$$r_{CH_4}\left[\text{kmol}\cdot\text{m}^{-3}\cdot\text{s}^{-1}\right]=2.119\times10^{11}\cdot\exp\left[-\frac{2.027\times10^8}{RT}\right]\cdot\left[CH_4\right]^{0.2}\cdot\left[O_2\right]^{1.3}, \quad (7)$$

where the unit of reaction rate is the kmol/(m^3·s), the unit of activation energy is J/kmol, and the unit of concentration is kmol/m^3. This chemical kinetic model can be used to accurately describe flame dynamics and flame responses to external perturbations [44]. Thermal effects can be relatively well captured by the chemical kinetic model.

2.4. Design parameters

The primary focus of the present study is placed on determining essential factors that affect the combustion stability of the systems. The design parameters of the combustion systems are summarized in Table 1 with the computational fluid dynamics modeling. The influences are investigated by varying a particular design parameter while maintaining the other design parameters.

Table 1. Design parameters of the millimeter-scale cavity-stabilized combustion systems used in the computational fluid dynamics modeling

Variables	Inlet velocity (m/s)	Equivalence ratio	Thermal conductivity (W/(m·K))	Channel height (mm)	Heat transfer coefficient (W/(m^2·K))
Effect of thermal conductivity	0.3	1.0	0.5, 1.4, 50, 50-0.5, 200	0.3	10
Effect of equivalence ratio	0.3	0.4, 0.6, 0.8, 1.0, 1.2	1.4	0.3	10
Effect of inlet velocity	0.1, 0.3, 0.5, 0.7	1.0	1.4	0.3	10
Effect of heat transfer coefficient	0.3	1.0	1.4	0.3	10, 20, 40, 60
Effect of channel height	0.3	1.0	1.4	0.3, 0.4, 0.5	10

2.5. Validation of the model

Validation of the computerized model is conducted during the development of the model with the

ultimate goal of producing an accurate and credible model. Validation checks the accuracy of the model's representation of the real system. Model validation is defined to mean "substantiation that a computerized model within its domain of applicability possesses a satisfactory range of accuracy consistent with the intended application of the model". To verify the accuracy of the model, the predictions are compared with the data obtained from experimental measurements. A constant fuel-air stoichiometry is maintained in operation. The fluid centerline temperature is plotted in Figure 2 against the streamwise distance. The fluid centerline temperature profiles are determined from thermographic measurements and predicted by the model. The predictions are in satisfactory agreement with the data obtained from experimental measurements.

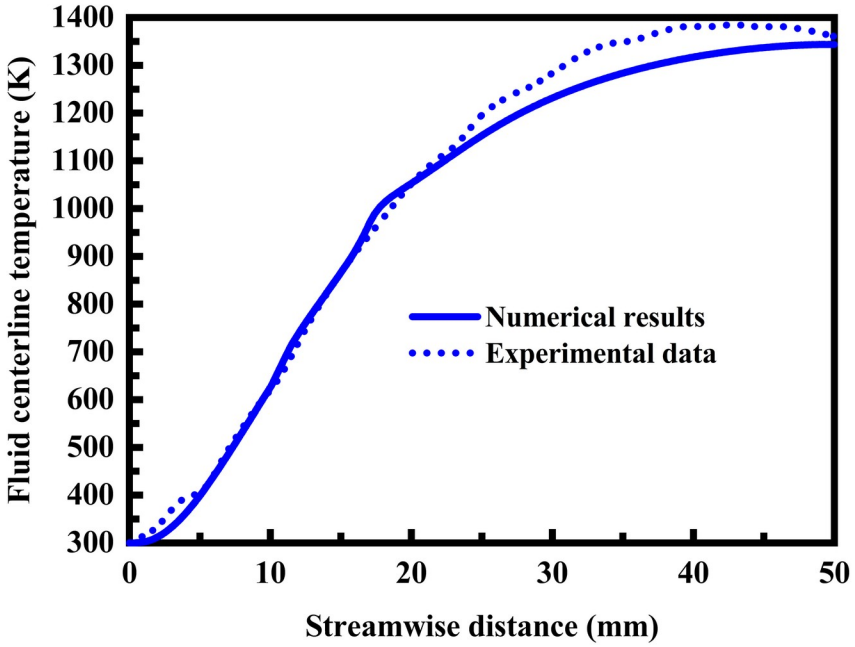

Figure 2. Fluid centerline temperature profiles determined from thermographic measurements and predicted by the model. A constant fuel-air stoichiometry is maintained in operation. Stoichiometry is the determination of the proportions in which elements or compounds react with one another. The rules followed in the determination of stoichiometric relationships are based on the laws of conservation of mass and energy and the law of combining weights or volumes.

3. Results and discussion

3.1. Performance comparison

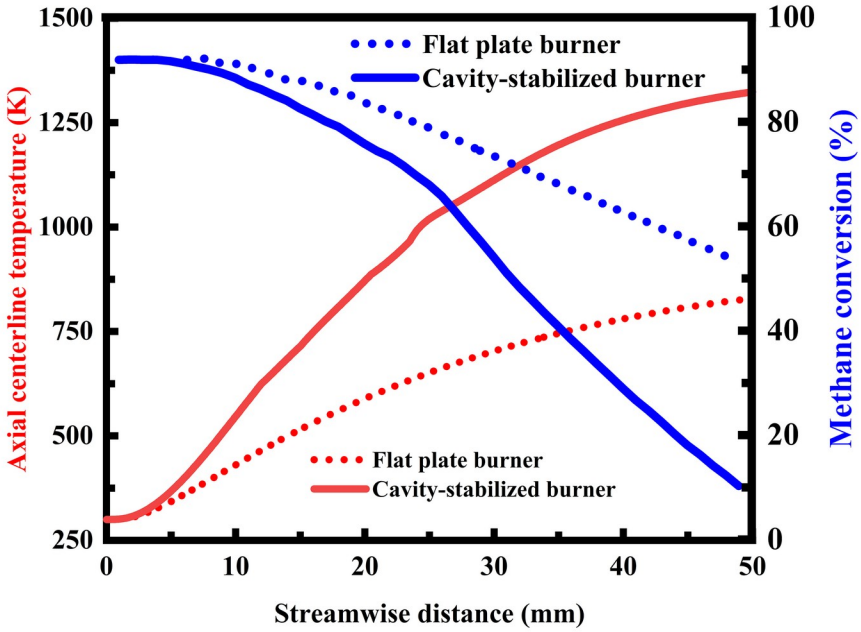

Figure 3. Axial fluid centerline temperature and methane mass fraction profiles along the length of the flat-plate and cavity-stabilized burners.

Prior to performing the computation, a comparison of methane conversion rate is carried out between a flat-plate burner and a cavity-stabilized burner. The composition change of the flat-plate burner and the cavity-stabilized burner is determined under the conditions of an equivalence ratio of 1.0, an inlet velocity of 0.5 m/s, and a wall thermal conductivity of 0.7 W/(m·K). The results are present in Figure 3, in which the axial fluid centerline temperature and the methane mass fraction are plotted against the streamwise distance. The methane conversion rate of the flat-plate burner is about 30%, and the methane conversion rate of the cavity-stabilized burner is about 90%. Therefore, the combustion efficiency of methane in the cavity-stabilized burner is higher than that of methane in the flat-plate burner. More complete combustion can be achieved in the cavity-stabilized burner. Even after ignition, it is difficult to maintain stable combustion in the flat-plate burner.

When the cavity structure is formed, a recirculation region is established for the cavity-stabilized burner. As a result, the methane mass fraction is small at the outlet, and the axial fluid centerline temperature is higher than that in the flat-plate burner. Therefore, the cavity structure plays a vital role in the combustion performance and efficiency of the burner, and the cavity-stabilized burner operates at a substantially higher temperature than the flat-plate burner. The contour plots of temperature are illustrated in Figure 4 for the flat-plate and cavity-stabilized burners. An important feature of the cavity-stabilized burner is that high enough flame temperatures are achievable to permit effective use of the fuel, thereby raising the temperature to about 1400 K, which is much higher than that in the flat-plate burner. Inasmuch as temperature and reaction rate are functionally related, an increase in temperature will lead to a corresponding increase in the rate of the combustion reaction. As a result, rapid, efficient thermal combustion occurs in the cavity-stabilized burner. Combustion of the methane-air mixture is stabilized in the cavities. The combustion region is maintained downstream of the cavity structure, which is capable of creating a recirculation region to provide heat to the mixture either through conduction or radiation. This differs from the flat-plate burner in which the cavities are absence. Advantageously, the cavity structure is useful for flame stabilization applications. The temperature increases when cavity stabilization is used. Combustion is stabilized by recirculation of hot combustion products induced by the cavity structure. However, the cavity-stabilized burner has practical limits in terms of the cavity structure, since complexity is introduced into the design of the cavity-stabilized combustion system.

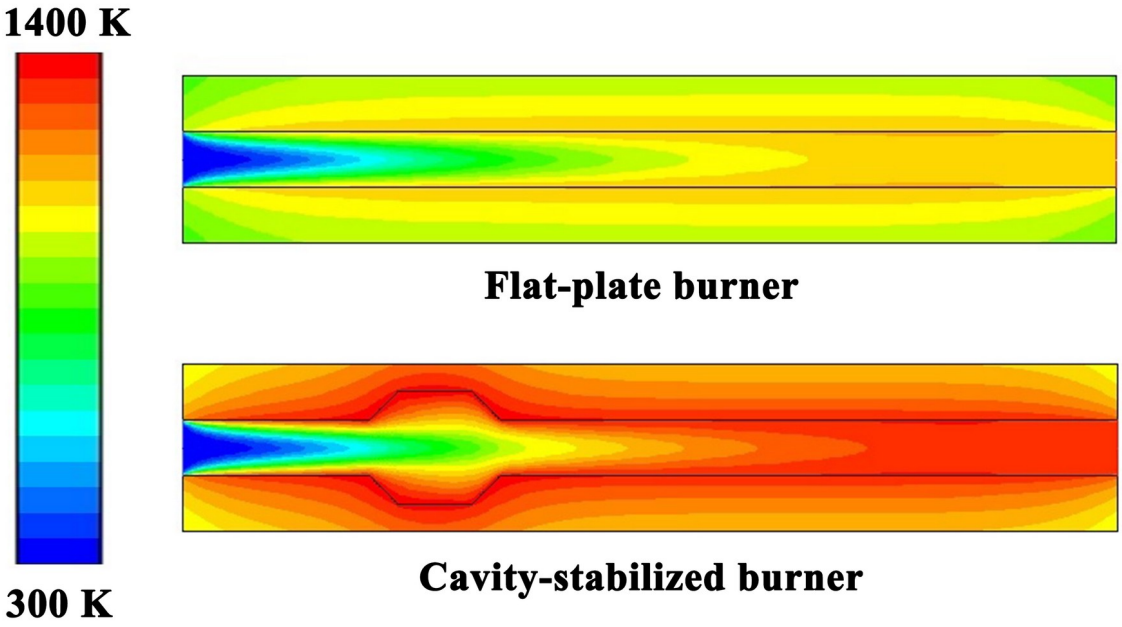

Figure 4. Contour plots of temperature for the flat-plate and cavity-stabilized burners. At room temperature, the thermal conductivity of the burner walls is 1.4 W/(m·K).

3.2. Effect of inlet velocity

The effect of changes in methane-air mixture inlet velocity on burner temperature changes is investigated, and the axial fluid centerline temperature profiles are presented in Figure 5 along the length of the cavity-stabilized burner under different methane-air mixture inlet velocity conditions. Additionally, the effect of changes in methane-air mixture inlet velocity on methane conversion is illustrated in Figure 6 at the outlet of the cavity-stabilized burner. With the increase of the inlet velocity, the residence time of the fuel in the cavity-stabilized burner becomes shorter. As the methane-air mixture inlet velocity increases, the position of the ignition point of the burner gradually moves away from the inlet to the outlet, as presented in Figure 5 by the axial fluid centerline temperature profiles. This will lead to raise the temperature to about 1400 K, which is much lower than the adiabatic flame temperature but may lead to significant formation of nitrogen oxides.

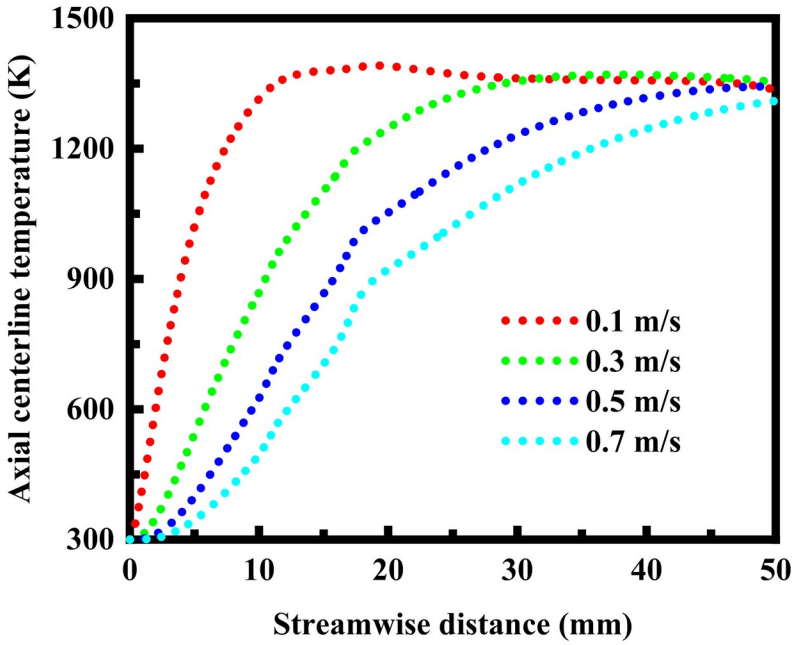

Figure 5. Axial fluid centerline temperature profiles along the length of the cavity-stabilized burner

under different methane-air mixture inlet velocity conditions.

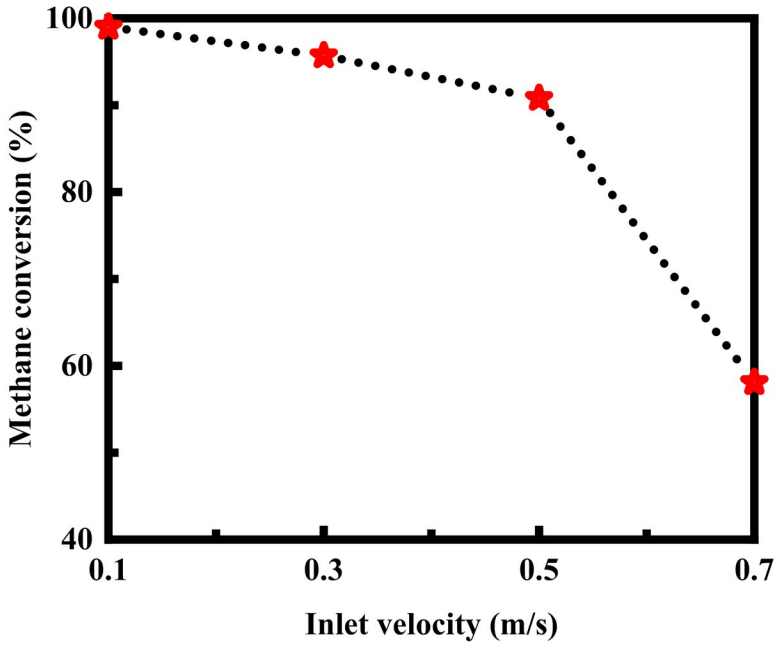

Figure 6. Effect of methane-air mixture inlet velocity on the methane conversion at the outlet of the cavity-stabilized burner.

In addition, the methane conversion rate increases with the decrease of the methane-air mixture inlet velocity, as illustrated in Figure 6 by the effect of methane-air mixture inlet velocity, thereby stabilizing combustion. Combustion is more readily stabilized in the cavity-stabilized burner at low inlet velocities. Blowout will occur at sufficiently high inlet velocities [45, 46]. Therefore, an appropriate inlet velocity of the methane-air mixture is very important for continuous stabilization of combustion in the cavity-stabilized burner. Cavity-stabilized combustion will tend to reduce unburned hydrocarbons emissions, as illustrated in Figure 6 by the effect of methane-air mixture inlet velocity. Consequently, the inlet velocity of the mixture is a critical factor in assuring flame stability within the cavity-stabilized burner. There is a narrow range of inlet velocities that permit sustained combustion within the cavity-stabilized burner.

The axial centerline rate profiles of the combustion reaction are presented in Figure 7 under different methane-air mixture inlet velocity conditions. As the inlet flow velocity increases, the peak of the reaction rate along the axis gradually moves away from the inlet to the outlet. When the methane-air mixture inlet velocity is low, methane is substantially completely converted near the inlet, and the peak of the reaction rate is also close to the inlet. When the methane-air mixture inlet velocity is high, the flame shifts toward the outlet, and the fuel fails to fully react with air, as presented in Figure 7 by the axial centerline rate profiles. In this case, the peak of the reaction rate is closer to the outlet.

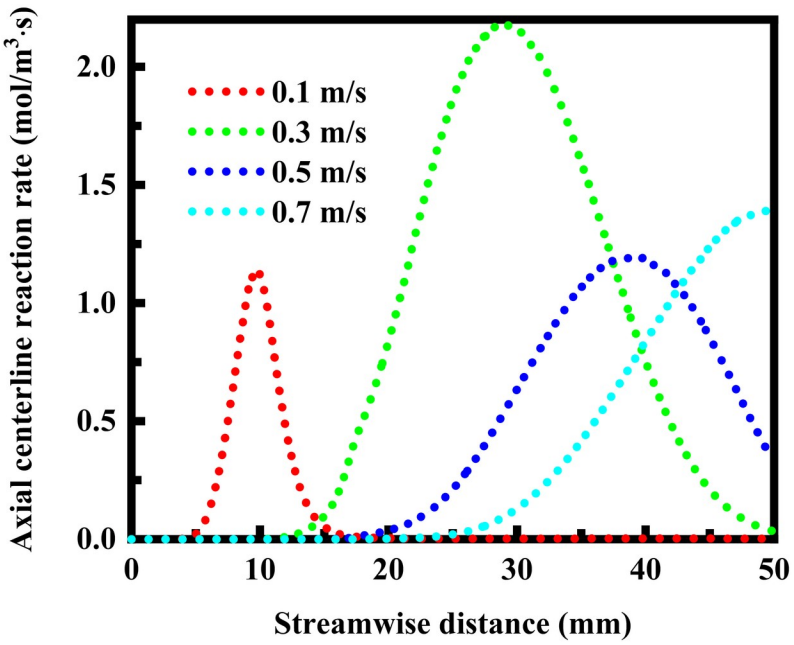

Figure 7. Axial centerline rate profiles of the combustion reaction in the cavity-stabilized burner under different methane-air mixture inlet velocity conditions.

The transverse rate profiles of the combustion reaction are presented in Figure 8 at different distances from the axial centerline. The methane-air mixture inlet velocity is 0.3 m/s. When the distance from the axial centerline is 0.5 mm and 1.0 mm, the peak of the reaction rate generally occurs near the middle of the cavity-stabilized burner. When the position is near the inner wall surface, the peak of the reaction rate is close to the entrance of the cavity-stabilized burner. This is because when the velocity of the methane-air mixture is low at the inlet of the cavity-stabilized burner, the wall temperature is higher than the temperature of the central flow channel, and the gas near the wall can quickly absorb heat and reach the ignition temperature to react. The irregular change of the rate of the combustion reaction near the cavities is mainly due to the formation of low-speed recirculation regions, in which the heat and mass transfer in the cavities are uneven. Advantageously, the recirculation regions make the gas in the cavities flow violently, which facilitates the combustion process. The vortex flow which arises bursts open at a sudden change of cross section, with the initiation of a back-flow zone which serves to stabilize a flame in the operation of the burner.

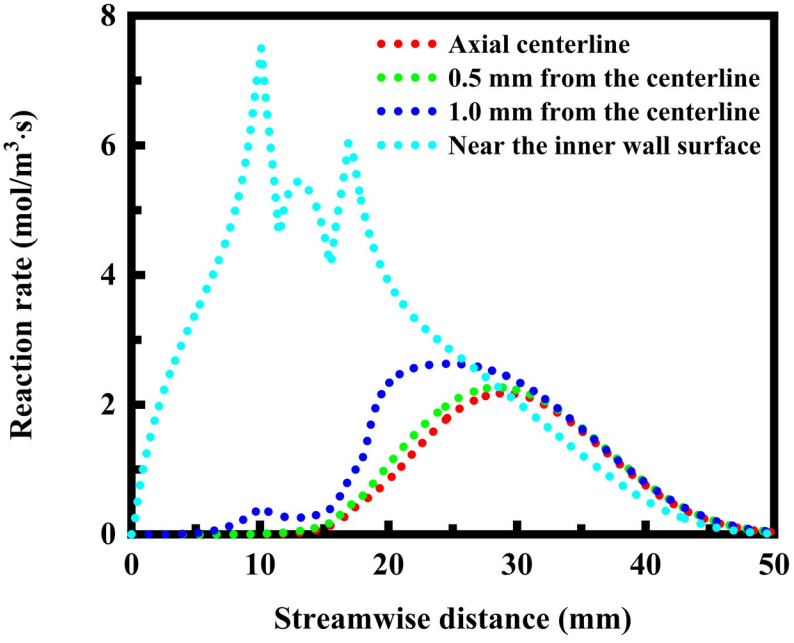

Figure 8. Transverse rate profiles of the combustion reaction at different distances from the axial centerline. The methane-air mixture inlet velocity is 0.3 m/s.

3.3. Effect of channel height

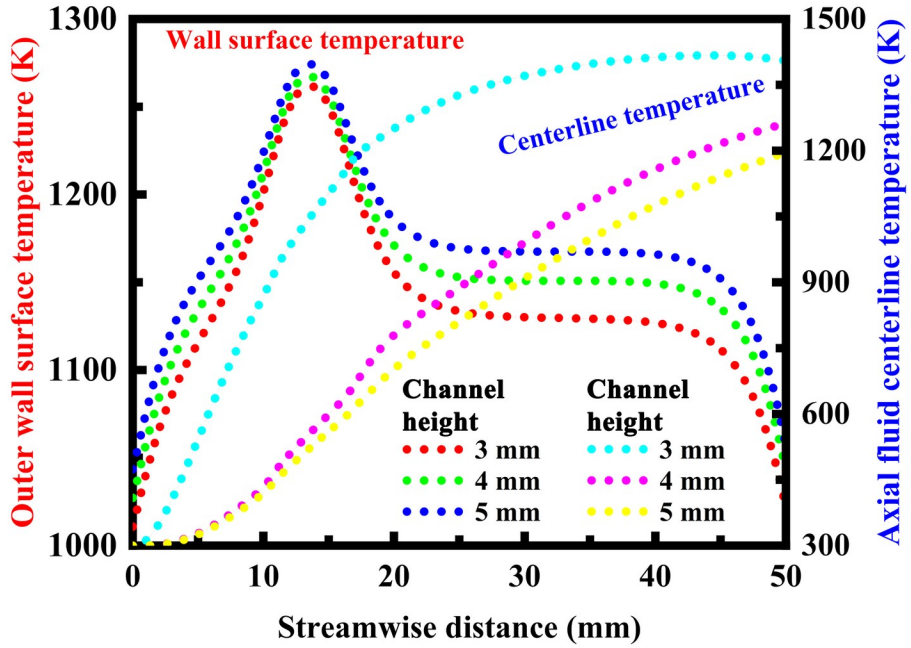

Figure 9. Temperature profiles along the outer wall surface of the cavity-stabilized burner and along the axial centerline under different channel height conditions.

The major problem of micro-structured combustion systems is the high ratio of surface to volume [47, 48]. As the ratio of surface to volume increases, heat loss to the surroundings increases, which could eventually lead to flame quenching [49, 50]. Therefore, the effect of the dimensions of the burner, for example, channel height, is investigated to better understand the stability of flame in the cavity-stabilized burner. The change characteristics of the temperature along the outer wall surface of the burner and along the axial centerline are presented in Figure 9 under different channel height conditions. As the height of the burner channel increases, the temperature of the axial centerline of the burner decreases, and the ignition position of the flame is far away from the inlet position, which further reduces the combustion efficiency. As the height of the burner channel increases, the temperature of the outer wall increases. This is because under the same conditions such as a flow velocity of 0.3 m/s and an equivalence ratio of 1.0, the amount of methane flowing into the channel per unit time increases with the channel height. As a result, the heat released by fuel combustion increases, and the temperature of the outer wall surface increases. However, the combustion efficiency decreases with the channel height. As the height of the burner channel increases, the amount of unreacted fuel in the axial centerline becomes larger, and the premixed incoming fuel-air mixture will absorb more heat for preheating. As a result, the temperature of the axial centerline drops significantly.

3.4. Effect of wall thermal conductivity

The temperature change characteristics of the outer wall surface of the burner are illustrated in Figure 10 under different thermal conductivity conditions. As the thermal conductivity of the burner walls increases, the temperature of the outer wall surface increases and the wall temperature distribution is more uniform. Ceramics with a high thermal conductivity may be employed for the cavity-stabilized burner. However, excessive temperature will cause a large amount of heat loss, which will cause unstable combustion performance. In addition, it is important to operate the burner at a safe temperature. When the thermal conductivity of the burner walls is low, the temperature of the outer wall surface is also low and the temperature distribution is uneven. This will be detrimental to the flame

stability of the burner, and local thermal stress is prone to occur. In order to better solve the above problems, walls with anisotropic thermal conductivity can not only transfer heat upstream for preheating the low-temperature unreacted pre-mixed gas, but also reduce the large heat loss caused by excessive wall temperatures, which will lead to unstable combustion performance. Two-dimensional materials may have anisotropic thermal properties [51, 52], for example, graphene.

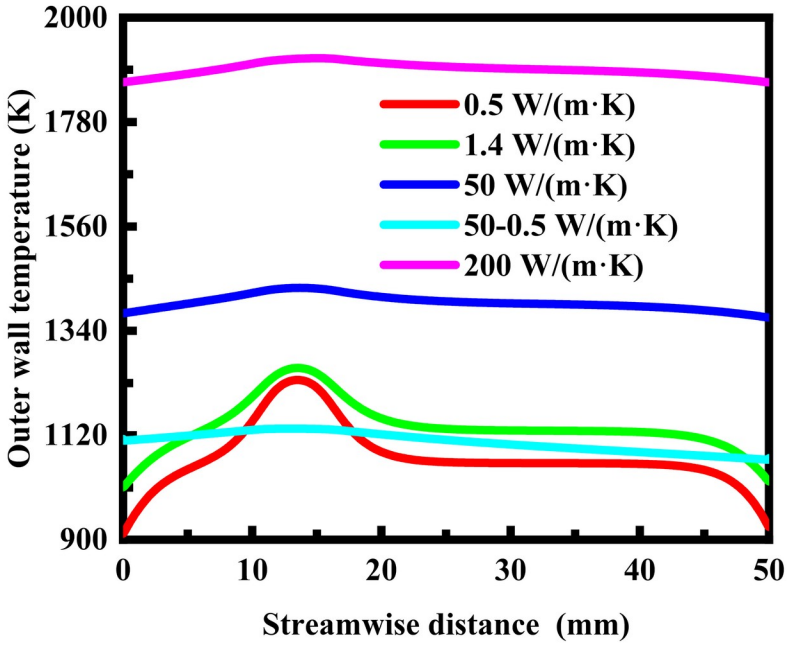

Figure 10. Temperature profiles along the outer wall surface of the cavity-stabilized burner under different thermal conductivity conditions.

The temperature profiles along the axial fluid centerline of the cavity-stabilized burner are presented in Figure 11 under different thermal conductivity conditions. The thermal conductivity of the burner walls mainly affects the temperature of the burner wall surfaces as well as the rate of heat transfer, as discussed above. In contrast, the thermal conductivity of the burner walls has little effect on the temperature along the axial centerline, as illustrated in Figure 11 by the temperature profiles along the outer wall surface of the cavity-stabilized burner. However, walls with excessively large thermal conductivity may cause unstable combustion, large heat loss, and the methane flame moves toward the outlet. Additionally, the temperature along the axial fluid centerline is relatively low when the thermal conductivity of the burner walls is 200 W/(m·K), as illustrated in Figure 11 by the temperature profiles along the outer wall surface of the cavity-stabilized burner, but the temperature at the outlet is relatively high. The difference in temperature is small between the different thermal conductivity cases, except the highest thermal conductivity case. Further improvements are achievable by using walls with anisotropic thermal conductivity, as discussed above.

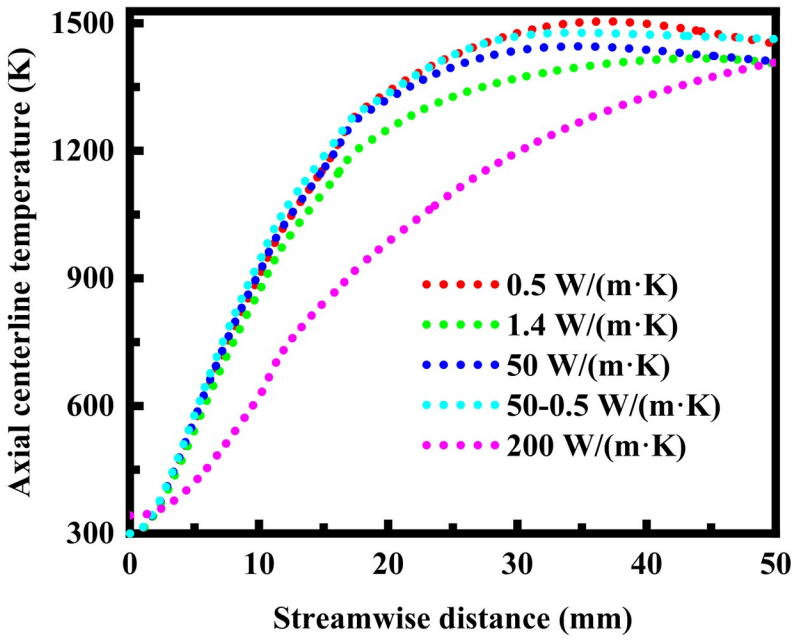

Figure 11. Temperature profiles along the axial fluid centerline of the cavity-stabilized burner under different thermal conductivity conditions.

3.5. Effect of wall heat transfer coefficient

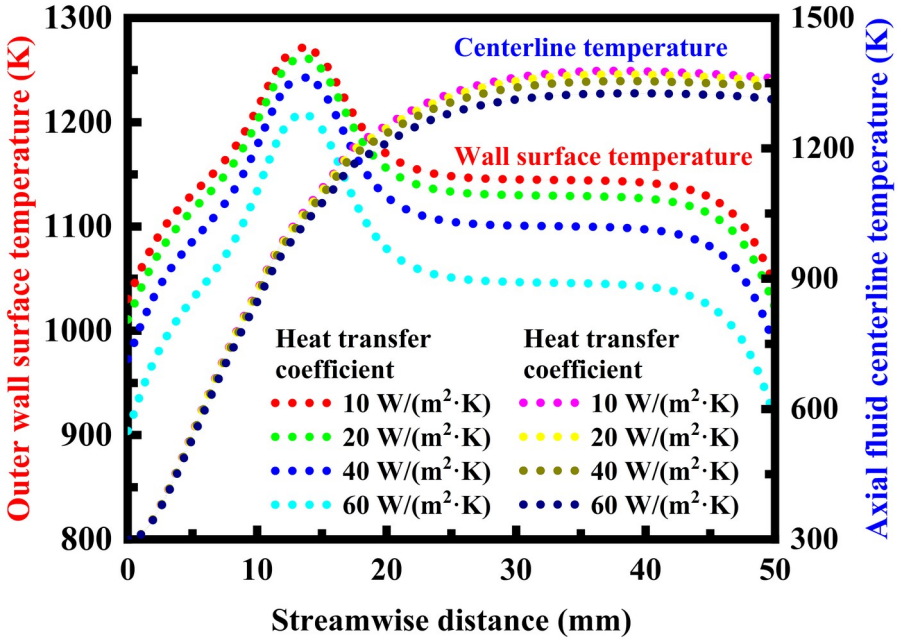

Figure 12. Temperature profiles along the outer wall surface of the burner and along the axial centerline under different wall heat transfer coefficient conditions.

The change characteristics of the temperature along the outer wall surface of the burner and along the axial fluid centerline are presented in Figure 12 under different wall heat transfer coefficient conditions. As the heat transfer coefficient between the solid surface and the environment is increased, the wall heat loss increases. As a result, both the temperature of the outer wall surface of the burner and the temperature along the axial fluid centerline decrease, which will lead to a drop in overall burner temperature, thereby reducing the combustion efficiency of the fuel. When the heat transfer coefficient between the solid surface and the environment is 10 W/(m^2·K), the highest temperatures are obtained at the outer wall surface and along the axial fluid centerline. With the increase of the heat transfer coefficient, the temperature of the outer wall surface decreases. At larger heat transfer coefficients, the

drop in temperature become more pronounced. The difference in temperature between the axial fluid centerlines is much smaller than that in temperature between the outer wall surfaces. For example, near the cavities where the axial distance varies from 10 to 20 mm, the maximum difference is about 40 K between the axial fluid centerline temperatures, but the maximum difference is about 90 K between the outer wall surface temperatures. Therefore, the wall heat transfer coefficient has a small effect on the axial fluid centerline temperature, but it plays a consider role in the outer wall surface temperature.

The variation characteristics of the combustion reaction rate along the axial centerline are illustrated in Figure 13 under different wall heat transfer coefficient conditions. As the heat transfer coefficient increases, the rate of the combustion reaction in the burner decreases due to increased heat losses from the outer wall surfaces, especially under very lager wall heat transfer coefficient conditions. However, the peak rate of the combustion reaction remains unchanged, regardless of the wall heat transfer coefficient. Therefore, losses of combustion stability because of heat losses are a main issue that requires careful management of thermal energy for the burner. A means for thermal management should be provided. From a practical viewpoint, the walls of the cavity-stabilized burner should have a thermal conductivity that is anisotropic. The burner walls should inhibit transverse heat conduction but allow axial heat conduction. These burner walls with anisotropic heat conduction properties will allow upstream heat flux to preheat the incoming mixture, yet not allow heat losses in the transverse direction. Alternatively, different suggestions have been made for facilitating the stability of flame in micro-structured combustion systems [53, 54]. To overcome the problem of heat losses involved in micro-structured combustion systems, catalytic combustion has been demonstrated the advantages in terms of reduced heat losses [55, 56]. This approach can substantially eliminate the formation of oxides of nitrogen [57, 58] and greatly reduce heat loss, but surface transport is still a problem. Catalytically supported thermal combustion, which is a unique combination of catalytic and gas phase combustion, can achieve higher stability and obtain higher efficiency in operation than otherwise obtainable, since combustion is no longer limited by mass transfer.

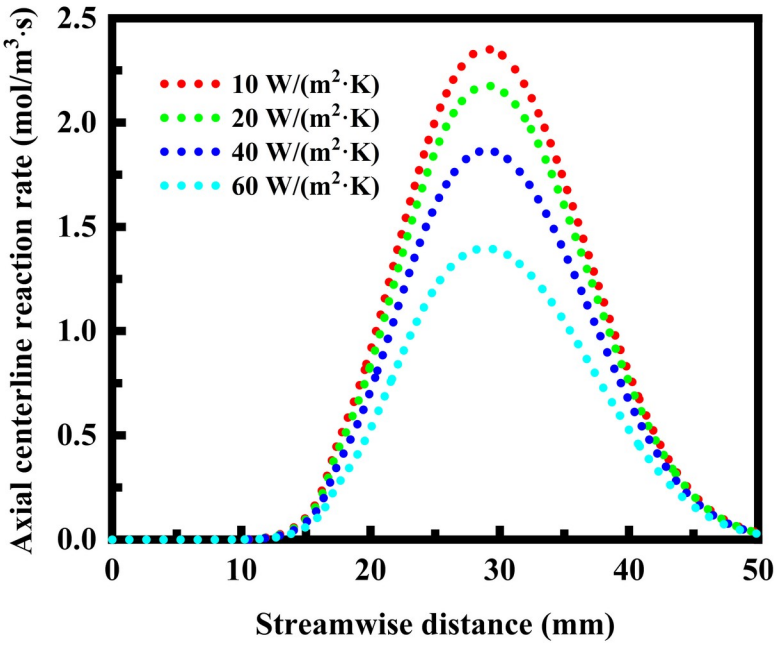

Figure 13. Axial centerline rate profiles of the combustion reaction under different wall heat transfer coefficient conditions.

3.6. Effect of fuel-air equivalence ratio

Combustion instability is generally understood as high amplitude pressure oscillations that occur within the combustion chamber due to the turbulent nature of the combustion process and large

volumetric energy release within the closed cavity of the combustion chamber. Many factors may contribute to a stable or an unstable state within the combustion chamber, including the fuel content, fuel and air injection speed or inlet pressure, fuel-air concentration, temperature changes within the combustion chamber, and the stability of the flame. Operating instabilities may further be amplified by the physical mechanisms of a particular combustion system design. The effect of fuel-air equivalence ratio on the temperature profiles is investigated along the outer wall surface of the cavity-stabilized burner and along the axial fluid centerline under different wall heat transfer coefficient conditions.

The temperature profiles along the outer wall surface of the cavity-stabilized burner and along the axial fluid centerline are presented in Figure 14 under different fuel-air equivalence ratio conditions. As the fuel-air equivalence ratio increases to up 1.0, both the temperature along the axial fluid centerline and the temperature along the outer wall surface gradually increase. The amount of heat released by the combustion reaction increases due to the increased amount of the methane gas flowing into the cavity-stabilized burner. This is because when the fuel-air equivalence ratio is less than 1.0, the amount of the methane gas flowing into the cavity-stabilized burner per unit time is smaller than that in the case of complete combustion in which the fuel-air equivalence ratio is 1.0. However, when the fuel-air equivalence ratio is increased from 1.0 to 1.2, both the temperature along the axial fluid centerline and the temperature along the outer wall surface decrease. This is because when the fuel-air equivalence ratio is greater than 1.0, the amount of the methane gas flowing into the cavity-stabilized burner per unit time is greater than that in the case of complete combustion in which the fuel-air equivalence ratio is 1.0. This will cause the relative content of oxygen gas required for complete combustion to decrease, resulting in insufficient combustion. In this case, incomplete combustion occurs, since there is not enough oxygen to allow methane to react completely in the cavity-stabilized burner. Therefore, when the fuel-air equivalence ratio is 1.0, higher temperatures can be achieved in the cavity-stabilized burner, associated with higher combustion performance.

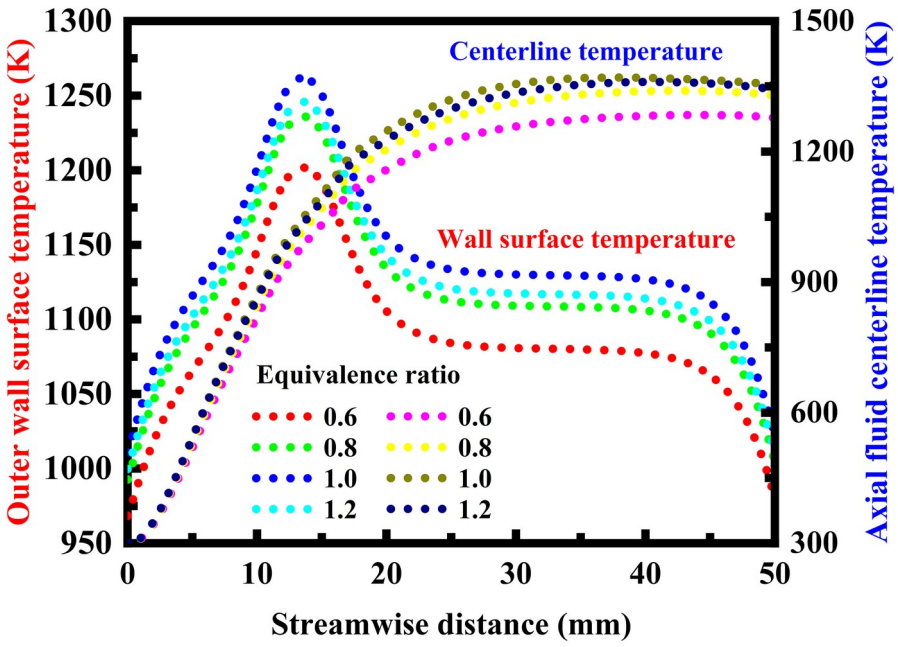

Figure 14. Temperature profiles along the outer wall surface of the cavity-stabilized burner and along the axial fluid centerline under different wall heat transfer coefficient conditions.

The effect of fuel-air equivalence ratio on the fluid temperature of the cavity-stabilized burner is investigated. The results are presented in Figure 15 with the stoichiometry indicated, in which the fluid temperature at the outlet is plotted against the fuel-air equivalence ratio. The fluid temperature at the outlet indicates the enthalpy of flue gas. The equivalence ratio can be fuel-lean or fuel-rich. Combustion has been stabilized at an equivalence ratio as small as 0.4. With lean premixed combustion, the fuel-air

equivalence ratio is smaller than 1.0. In this case, the fluid temperature at the outlet increases with the equivalence ratio of fuel to air, which increases power output of the cavity-stabilized burner. Use of an equivalence ratio of 1.0 permits complete combustion of the fuel, and therefore there is an optimum condition of maximal temperature. However, there is a dominant loss that is caused by sensible heat leaving with the flue gas. When the fuel-air equivalence ratio is greater than 1.0, the fluid temperature at the outlet decreases with the equivalence ratio of fuel to air, which is primarily caused by the amount of the methane gas flowing into the cavity-stabilized burner, as discussed above. In this case, the amount of air flowing into the cavity-stabilized burner is smaller than the amount of air required for complete combustion. Therefore, only a portion of the total fuel is reacted in the cavity-stabilized burner. For the fuel-rich case, there are issues of efficiency loss, since the equivalence ratio should be limited to allow sufficient air for combustion in the cavity-stabilized burner.

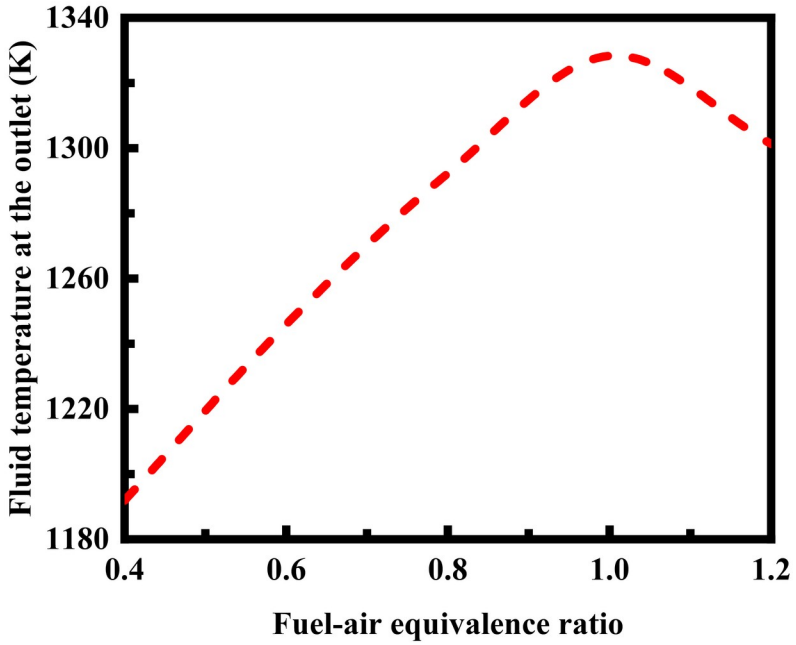

Figure 15. Effect of fuel-air equivalence ratio on the fluid temperature at the outlet of the cavity-stabilized burner with the stoichiometry indicated.

4. Conclusions

Computational fluid dynamics simulations are conducted to gain insights into the performance of the cavity-stabilized burner, such as reaction rates, species concentrations, temperatures, and flames.

Factors affecting combustion characteristics and flame stability are determined for the cavity-stabilized burner. The major conclusions are summarized as follows:

- Improvements in flame stability are achievable by using walls with anisotropic thermal conductivity. Such walls with anisotropic heat conduction properties will allow upstream heat flux to preheat the incoming mixture, yet not allow heat losses in the transverse direction.
- Loss of flame stability due to external heat losses are main issues that require thermal management. Heat-insulating materials are favored to minimize external heat losses.
- The thermal conductivity of the burner walls plays a vital role in flame stability. Burner walls with low thermal conductivity will cause hot spots, and burner walls with high thermal conductivity are substantially isothermal.
- There are issues of efficiency loss for fuel-rich cases.
- Burners with large dimensions lead to a delay in flame ignition and may cause blowout.
- The inlet velocity of the mixture is a critical factor in assuring flame stability within the cavity-

stabilized burner. There is a narrow range of inlet velocities that permit sustained combustion within the cavity-stabilized burner.

- Combustion is stabilized and flame stability is improved by recirculation of hot combustion products induced by the cavity structure.

References

[1] R.S. Wegeng and M.K. Drost. Developing new miniature energy systems. *Mechanical Engineering*, Volume 116, Issue 9, 1994, Pages 82-85.

[2] T.A. Ameel, R.O. Warrington, R.S. Wegeng, and M.K. Drost. Miniaturization technologies applied to energy systems. *Energy Conversion and Management*, Volume 38, Issues 10-13, 1997, Pages 969-982.

[3] A.H. Epstein. Millimeter-scale, micro-electro-mechanical systems gas turbine engines. *Journal of Engineering for Gas Turbines and Power*, Volume 126, Issue 2, 2004, Pages 205-226.

[4] R. Singh, A. Maity, and P.S.V. Nataraj. Dynamic modeling and robust nonlinear control of a laboratory gas turbine engine. *Aerospace Science and Technology*, Volume 126, 2022, Article Number: 107586.

[5] R.B. Peterson. Small packages. Miniaturization technologies applied to energy systems. *Mechanical Engineering*, Volume 123, Issue 06, 2001, Pages 58-61.

[6] S. Kota, G.K. Ananthasuresh, S.B. Crary, and K.D. Wise. Design and fabrication of microelectromechanical systems. *Journal of Mechanical Design*, Volume 116, Issue 4, 1994, Pages 1081-1088.

[7] S.A. Tadigadapa and N. Najafi. Developments in microelectromechanical systems (MEMS): A manufacturing perspective. *Journal of Manufacturing Science and Engineering*, Volume 125, Issue 4, 2003, Pages 816-823.

[8] G.K. Ananthasuresh and L.L. Howell. Mechanical design of compliant microsystems-A perspective and prospects. *Journal of Mechanical Design*, Volume 127, Issue 4, 2005, Pages 736-7383.

[9] J. E, J. Ding, J. Chen, G. Liao, F. Zhang, and B. Luo. Process in micro-combustion and energy conversion of micro power system: A review. *Energy Conversion and Management*, Volume 246, 2021, Article Number: 114664.

[10] J. E, B. Luo, D. Han, J. Chen, G. Liao, F. Zhang, and J. Ding. A comprehensive review on performance improvement of micro energy mechanical system: Heat transfer, micro combustion and energy conversion. *Energy*, Volume 239, Part E, 2022, Article Number: 122509.

[11] J. Wan and A. Fan. Recent progress in flame stabilization technologies for combustion-based micro energy and power systems. *Fuel*, Volume 286, Part 2, 2021, Article Number: 119391.

[12] A. Gharehghani, K. Ghasemi, M. Siavashi, and S. Mehranfar. Applications of porous materials in combustion systems: A comprehensive and state-of-the-art review. *Fuel*, Volume 304, 2021, Article Number: 121411.

[13] Y. Ju and K. Maruta. Microscale combustion: Technology development and fundamental research. *Progress in Energy and Combustion Science*, Volume 37, Issue 6, 2011, Pages 669-715.

[14] S.K. Chou, W.M. Yang, K.J. Chua, J. Li, and K.L. Zhang. Development of micro power generators - A review. *Applied Energy*, Volume 88, Issue 1, 2011, Pages 1-16.

[15] J. Kim, J. Yu, S. Lee, A. Tahmasebi, C.-H. Jeon, and J. Lucas. Advances in catalytic hydrogen combustion research: Catalysts, mechanism, kinetics, and reactor designs. *International Journal of Hydrogen Energy*, Volume 46, Issue 80, 2021, Pages 40073-40104.

[16] D.C. Walther and J. Ahn. Advances and challenges in the development of power-generation systems

at small scales. *Progress in Energy and Combustion Science*, Volume 37, Issue 5, 2011, Pages 583-610.

[17] J. Miwa, Y. Asako, C. Hong, and M. Faghri. Performance of gas-to-gas micro-heat exchangers. *Journal of Heat Transfer*, Volume 131, Issue 5, 2009, Article Number: 051801.

[18] C. Marques and K.W. Kelly. Fabrication and performance of a pin fin micro heat exchanger. *Journal of Heat Transfer*, Volume 126, Issue 3, 2004, Pages 434-444.

[19] Z. Zhao, Z. Zuo, W. Wang, N. Kuang, and P. Xu. Experimental studies on a high performance thermoelectric system based on micro opposed flow porous combustor. *Energy Conversion and Management*, Volume 253, 2022, Article Number: 115157.

[20] S.M.R. Sadatakhavi, S. Tabejamaat, M.E.A. Zade, B. Kankashvar, and M.R. Nozari. Numerical and experimental study of the effects of fuel injection and equivalence ratio in a can micro-combustor at atmospheric condition. *Energy*, Volume 225, 2021, Article Number: 120166.

[21] J. Guan, X. Lv, C. Spataru, and Y. Weng. Experimental and numerical study on self-sustaining performance of a 30-kW micro gas turbine generator system during startup process. *Energy*, Volume 236, 2021, Article Number: 121468.

[22] J.M. Seo, H.-S. Lim, J.Y. Park, M.R. Park, and B.S. Choi. Development and experimental investigation of a 500-W class ultra-micro gas turbine power generator. *Energy*, Volume 124, 2017, Pages 9-18.

[23] I.A. Waitz, G. Gauba, and Y.-S. Tzeng. Combustors for micro-gas turbine engines. *Journal of Fluids Engineering*, Volume 120, Issue 1, 1998, Pages 109-117.

[24] C.M. Spadaccini, A. Mehra, J. Lee, X. Zhang, S. Lukachko, and I.A. Waitz. High power density silicon combustion systems for micro gas turbine engines. *Journal of Engineering for Gas Turbines and Power*, Volume 125, Issue 3, 2003, Pages 709-719.

[25] O. Dessornes, S. Landais, R. Valle, A. Fourmaux, S. Burguburu, C. Zwyssig, and Z. Kozanecki. Advances in the development of a microturbine engine. *Journal of Engineering for Gas Turbines and Power*, Volume 136, Issue 7, 2014, Article Number: 071201.

[26] M. Nozari, S. Tabejamaat, H. Sadeghizade, and M. Aghayari. Experimental investigation of the effect of gaseous fuel injector geometry on the pollutant formation and thermal characteristics of a micro gas turbine combustor. *Energy*, Volume 235, 2021, Article Number: 121372.

[27] D.H. Lee, D.-E. Park, E. Yoon, and S. Kwon. A MEMS piston-cylinder device actuated by combustion. *Journal of Heat Transfer*, Volume 125, Issue 3, 2003, Pages 487-493.

[28] E. Lin, C.T. Wilson, A. Leroy, and B.E. Fil. High energy density entrainment-based catalytic micro-combustor for portable devices. *Energy Conversion and Management*, Volume 285, 2023, Article Number: 117014.

[29] N.S. Kaisare and D.G. Vlachos. A review on microcombustion: Fundamentals, devices and applications. *Progress in Energy and Combustion Science*, Volume 38, Issue 3, 2012, Pages 321-359.

[30] K. Maruta. Micro and mesoscale combustion. *Proceedings of the Combustion Institute*, Volume 33, Issue 1, 2011, Pages 125-150.

[31] D. Dunn-Rankin, E.M. Leal, and D.C. Walther. Personal power systems. *Progress in Energy and Combustion Science*, Volume 31, Issues 5-6, 2005, Pages 422-465.

[32] A.C. Fernandez-Pello. Micropower generation using combustion: Issues and approaches. *Proceedings of the Combustion Institute*, Volume 29, Issue 1, 2002, Pages 883-899.

[33] K.M. Lyons. Toward an understanding of the stabilization mechanisms of lifted turbulent jet flames: Experiments. *Progress in Energy and Combustion Science*, Volume 33, Issue 2, 2007, Pages 211-231.

[34] S.J. Shanbhogue, S. Husain, and T. Lieuwen. Lean blowoff of bluff body stabilized flames: Scaling

and dynamics. *Progress in Energy and Combustion Science*, Volume 35, Issue 1, 2009, Pages 98-120.

[35] J. Choi, W. Lee, R. Rajasegar, T. Lee, and J. Yoo. Effects of hydrogen enhancement on mesoscale burner array flame stability under acoustic perturbations. *International Journal of Hydrogen Energy*, Volume 46, Issue 74, 2021, Pages 37098-37107.

[36] K.R. McManus, T. Poinsot, and S.M. Candel. A review of active control of combustion instabilities. *Progress in Energy and Combustion Science*, Volume 19, Issue 1, 1993, Pages 1-29.

[37] R. Sadanandan, A. Chakraborty, V.K. Arumugam, and S.R. Chakravarthy. Partially premixed flame stabilization in the presence of a combined swirl and bluff body influenced flowfield: An experimental investigation. *Journal of Engineering for Gas Turbines and Power*, Volume 142, Issue 7, 2020, Article Number: 071010.

[38] K.M. Kundu, D. Banerjee, and D. Bhaduri. On flame stabilization by bluff-bodies. *Journal of Engineering for Gas Turbines and Power*, Volume 102, Issue 1, 1980, Pages 209-214.

[39] C.C. Rasmussen, J.F. Driscoll, K.-Y. Hsu, J.M. Donbar, M.R. Gruber, and C.D. Carter. Stability limits of cavity-stabilized flames in supersonic flow. *Proceedings of the Combustion Institute*, Volume 30, Issue 2, 2005, Pages 2825-2833.

[40] N. Kato and S.-K. Im. Flame dynamics under various backpressures in a model scramjet with and without a cavity flameholder. *Proceedings of the Combustion Institute*, Volume 38, Issue 3, 2021, Pages 3861-3868.

[41] S. Wang and A. Fan. Combustion regimes of syngas flame in a micro flow reactor with controlled temperature profile: A numerical study. *Combustion and Flame*, Volume 230, 2021, Article Number: 111457.

[42] S. Ni, D. Zhao, Y. You, Y. Huang, B. Wang, and Y. Su. NOx emission and energy conversion efficiency studies on ammonia-powered micro-combustor with ring-shaped ribs in fuel-rich combustion. *Journal of Cleaner Production*, Volume 320, 2021, Article Number: 128901.

[43] C.K. Westbrook and F.L. Dryer. Simplified reaction mechanisms for the oxidation of hydrocarbon fuels in flames. *Combustion Science and Technology*, Volume 27, Issues 1-2, 1981, Pages 31-43.

[44] C.K. Westbrook and F.L. Dryer. Chemical kinetic modeling of hydrocarbon combustion. *Progress in Energy and Combustion Science*, Volume 10, Issue 1, 1984, Pages 1-57.

[45] D.G. Norton and D.G. Vlachos. Combustion characteristics and flame stability at the microscale: a CFD study of premixed methane-air mixtures. *Chemical Engineering Science*, Volume 58, Issue 21, 2003, Pages 4871-4882.

[46] D.G. Norton and D.G. Vlachos. A CFD study of propane-air microflame stability. *Combustion and Flame*, Volume 138, Issues 1-2, 2004, Pages 97-107.

[47] T.T. Leach and C.P. Cadou. The role of structural heat exchange and heat loss in the design of efficient silicon micro-combustors. *Proceedings of the Combustion Institute*, Volume 30, Issue 2, 2005, Pages 2437-2444.

[48] T.T. Leach, C.P. Cadou, and G.S. Jackson. Effect of structural conduction and heat loss on combustion in micro-channels. *Combustion Theory and Modelling*, Volume 10, Issue 1, 2006, Pages 85-103.

[49] C.-H. Chen and P.D. Ronney. Scale and geometry effects on heat-recirculating combustors. *Combustion Theory and Modelling*, Volume 17, Issue 5, 2013, Pages 888-905.

[50] N.S. Kaisare and D.G. Vlachos. Optimal reactor dimensions for homogeneous combustion in small channels. *Catalysis Today*, Volume 120, Issue 1, 2007, Pages 96-106.

[51] X. Xu, L.F.C. Pereira, Y. Wang, J. Wu, K. Zhang, X. Zhao, S. Bae, C.T. Bui, R. Xie, J.T.L. Thong, B.H. Hong, K.P. Loh, D. Donadio, B. Li, and B. Özyilmaz. Length-dependent thermal conductivity in suspended single-layer graphene. *Nature Communications*, Volume 5, 2014, Article Number:

3689.

[52] Z. Wei, Z. Ni, K. Bi, M. Chen, and Y. Chen. In-plane lattice thermal conductivities of multilayer graphene films. *Carbon*, Volume 49, Issue 8, 2011, Pages 2653-2658.

[53] W. Liu, L. Wang, S. Su, Z. Wu, Y. Guo, and K. Du. Study of the flame flow and combustion characteristics of pool fires around a bluff body in the ship engine room. *Case Studies in Thermal Engineering*, Volume 28, 2021, Article Number: 101514.

[54] Y. Huang, X. He, Y. Jin, H. Zhu, and Z. Zhu. Effect of non-uniform inlet profile on the combustion performance of an afterburner with bluff body. *Energy*, Volume 216, 2021, Article Number: 119142.

[55] Y. Yan, G. Wu, W. Huang, L. Zhang, L. Li, and Z. Yang. Numerical comparison study of methane catalytic combustion characteristic between newly proposed opposed counter-flow micro-combustor and the conventional ones. *Energy*, Volume 170, 2019, Pages 403-410.

[56] J.M. Rodrigues, M.F. Ribeiro, and E.C. Fernandes. Catalytic activity of electrodeposited cobalt oxide films for methane combustion in a micro-channel reactor. *Fuel*, Volume 232, 2018, Pages 51-59.

[57] J.A. Miller and C.T. Bowman. Mechanism and modeling of nitrogen chemistry in combustion. *Progress in Energy and Combustion Science*, Volume 15, Issue 4, 1989, Pages 287-338.

[58] R.W. Bilger. The structure of turbulent nonpremixed flames. *Symposium (International) on Combustion*, Volume 22, Issue 1, 1989, Pages 475-488.